Earth and Planetary Science Letters 280 (2009) 285–295

Contents lists available at ScienceDirect

Earth and Planetary Science Letters

journal homepage: www.elsevier.com/locate/epsl

Martian meteorite chronology and the evolution of the interior of Mars

Audrey Bouvier [a,b,*], Janne Blichert-Toft [a], Francis Albarède [a]

[a] Ecole Normale Supérieure de Lyon, UMR CNRS 5570, 46 Allée d'Italie, 69364 Lyon Cedex 07, France
[b] Arizona State University, School of Earth and Space Exploration, Tempe, AZ 85287-1404, USA

ARTICLE INFO

Article history:
Received 3 November 2008
Received in revised form 28 January 2009
Accepted 29 January 2009
Available online 26 February 2009

Editor: R.W. Carlson

Keywords:
Mars
SNC meteorites
ALH 84001
Pb–Pb dating
^{142}Nd
planetary differentiation

ABSTRACT

The Earth, Moon, and Mars are the only three planets for which satellite and ground observations can be confronted with extensive chronological and geochemical observations of rock samples. Here we use new Pb isotope data on shergottites, nakhlites, Chassigny, and the ALH 84001 orthopyroxenite to reassess chronological evidence and discuss its bearing on the evolution of the interior of Mars. We find that the depleted shergottites formed at 4.3 Ga, i.e., ~170 Ma after the last equilibration of pyroxene-rich cumulates with the magma ocean, while the younger enriched and intermediate shergottites, as well as ALH 84001, formed ~200 Ma later at ~4.1 Ga, after the residual part of the mantle had been largely mixed back into these cumulates. We also demonstrate that the Th/U ratios inferred from Pb isotopes require shergottite ages older than ~4.0 Ga. We finally reexamine the implications of this new chronological framework for the interpretation of ^{142}Nd and ^{182}W anomalies in Martian meteorites. We conclude that shergottites represent samples that derived from a volcanic basement subsequently shattered by the ~3.9 Ga Late Heavy Bombardment (LHB). Although the magmatic activity of Mars had strongly declined by the time of the LHB, the new chronology of Martian meteorites proposed here allows the Martian mantle to be convective until today. The 1.3 Ga old emplacement of nakhlites and chassignites corresponds to decompression melting of ilmenite-rich mantle domains and not to renewed global magmatic activity of the planet. With the exception of this event, the history of the interior of Mars therefore somewhat resembles that of the Moon.

1. Introduction

Isotope chronology on Apollo samples has permitted the cratering history of the Moon to be recast into absolute time (Hartmann, 1970). The extrapolation of this cratering history to Mars (Soderblom et al., 1974; Neukum and Wise, 1976) shed the first light on the history of the Martian surface by showing that the entire southern hemisphere of Mars was reshaped at about the time of the Late Heavy Bombardment (LHB) at 3.8–3.9 Ga by very large impacts (Barlow, 1988; Hartmann and Neukum, 2001). Although the northern hemisphere subsequently was covered until ~3.5 Ga by basins filled by presumably eolian deposits, the basement shows indications of large impacts of LHB age (Werner, 2008). The chronology of magmatic events on Mars and their relationship to both the surface age derived from crater counting and the structure and dynamics of the Martian mantle is the main focus of this work.

The chronological 'ground truth' provided by the Apollo and lunar meteorite samples for the Moon (Tera and Wasserburg, 1974) is missing for the SNC meteorites (Shergottite–Nakhlite–Chassignite meteorites, respectively gabbro, pyroxenite, and dunite rock types). Contrary to lunar samples with ages ranging from 3.0 to 4.5 Ga, the Rb–Sr, U–Pb, Sm–Nd, and Lu–Hf mineral isochrons of shergottites show much younger ages around 180, 475, and 575 Ma (Nyquist et al., 2001), while nakhlites and Chassigny are unambiguously found by all dating techniques, inclusive of U–Pb, to have crystallized at ~1.3 Ga (Nyquist et al., 2001). Only the ungrouped Martian meteorite ALH 84001 (an orthopyroxenite) yields an ancient 4.5 Ga Sm–Nd crystallization age (Jagoutz et al., 1994; Nyquist et al., 1995), older than any surface dated so far by crater densities (Werner, 2008). Moreover, there is no SNC that qualifies as a volcanic rock petrographically comparable to, for example, a Hawaiian-type basaltic lava flow. At face value, Martian meteorites seem to reflect intense magmatic activity of the planet's interior until recent times (Jones, 2003) (i.e., 100–600 Ma). In stark contrast to this observation stands the conundrum that most of the Martian surface is much older than even the nakhlite age (1.3 Ga) (Frey, 2006; Fritz et al., 2007). A limited number of recent volcanic areas, such as some late eruptions of Tharsis volcanoes (Hartmann and Neukum, 2001), are rare exceptions to this. Since the ages of extraction of these meteorites from Mars, as indicated by the length of time they have been exposed to cosmic rays, are multiple and range between 1 and 18 Ma (Nyquist et al., 2001), the challenge is to explain how the impactors responsible for the multiple SNC extractions have consistently found their way to such a minute fraction of the Martian surface. If SNC mineral ages are to be taken at face value, the recent internal activity of Mars is still substantial and yet this does not show up in crater-counting chronology.

* Corresponding author. Arizona State University, School of Earth and Space Exploration, Tempe, AZ 85287-1404, USA. Tel.: +1 480 965 7762; fax: +1 480 965 8102.
E-mail address: audrey.bouvier@asu.edu (A. Bouvier).

0012-821X/$ – see front matter © 2009 Elsevier B.V. All rights reserved.
doi:10.1016/j.epsl.2009.01.042

Table 1
Pb isotope compositions of Martian meteorites.

Meteorite name and chemical group	Sample and fraction	Residue weight (g)	Pb[a] (ppb)	Pb (ng)	Uncorr.[b] $^{206}Pb/^{204}Pb$	Corr.[c] $^{206}Pb/^{204}Pb$	Corr.[c] 2σ % err.	Corr.[c] $^{207}Pb/^{204}Pb$	Corr.[c] $^{208}Pb/^{204}Pb$	Corr.[c] $^{207}Pb/^{206}Pb$	Corr.[c] 2σ % err.
Basaltic shergottites											
NWA 480[e] enriched	Unleached whole-rock	0.115	466		16.4404	16.4391	0.0039	14.5577	36.4276	0.885552	0.0008
	Whole-rock R	0.066	106		15.7042	15.6831	0.0331	14.1888	35.5465	0.904720	0.0110
	L1			17		17.3468	0.0067	15.0068	37.4299	0.865086	0.0012
	L2			9		15.2705	0.0090	14.0017	35.1532	0.916913	0.0016
	L3			9		15.2176	0.0075	13.9653	35.0719	0.917694	0.0017
	Maskelynite R	0.032	273		15.3476	15.3032	0.0626	13.9357	35.0223	0.910638	0.0235
	L1			30		16.3785	0.0035	14.5918	36.2829	0.890912	0.0008
	L2			25		16.3605	0.0035	14.4696	36.3012	0.884435	0.0009
	Pyroxene R	0.154	32		14.4664	14.4643	0.0137	13.1904	34.2407	0.911925	0.0022
	L1			32		16.9469	0.0025	14.9597	36.8929	0.882741	0.0007
	L2			–		too low					
RBT 04262, 8[f] enriched	Whole-rock R	0.047	245		14.3695	14.3682	0.0105	13.5381	34.5086	0.942230	0.0020
	L1			6		16.8064	0.0256	13.5353	38.2194	0.805363	0.0032
	L2			5		14.2874	0.0117	13.4915	34.4746	0.944239	0.0032
	L3			9		14.2798	0.0077	13.4840	34.4785	0.944263	0.0012
	Maskelynite R	0.021	514		14.1601	14.1594	0.0125	13.4455	34.3224	0.949579	0.0035
	L2			23		14.1841	0.0025	13.4664	34.3564	0.949398	0.0011
	L3			2		14.1816	0.0282	13.4671	34.3499	0.949619	0.0063
	Pyroxene + Olivine R	0.022	33		14.2111	14.2009	0.0851	13.3928	34.3001	0.943097	0.0175
	L2			2		14.1935	0.0371	13.4150	34.3484	0.945150	0.0050
	L3			0.4		14.3558	0.1928	13.5031	34.5264	0.940606	0.0305
Olivine-phyric shergottite											
NWA 1068[g] intermediate	Whole-rock R	0.400	224		13.6276	13.6214	0.0021	13.1774	33.6768	0.967403	0.0005
	L1			74		15.7214	0.0024	14.1598	36.0060	0.900673	0.0005
	L2			98		13.6715	0.0015	13.2276	33.8106	0.967523	0.0007
	L3			20		13.7617	0.0021	13.2697	33.8968	0.964242	0.0006
Olivine-orthopyroxene shergottite											
NWA 1195[h] depleted	Whole-rock R	0.549	16		12.0913	12.0888	0.0097	11.9335	32.0708	0.987159	0.0039
	L1			10		16.5171	0.0125	14.3258	36.5608	0.867304	0.0020
	L2			9		12.0116	0.0095	11.9007	32.0367	0.990732	0.0019
	L3			8		11.7777	0.0063	11.7578	31.8150	0.998340	0.0031
Nakhlites											
Y-000593, 53[i]	Unleached whole-rock	0.373	645		11.8049	11.8039	0.0025	11.5807	32.0117	0.981094	0.0008
	Whole-rock R	0.371	152		11.5948	11.5902	0.0083	11.5487	31.5386	0.996412	0.0031
	L1			223		12.0290	0.0016	11.6158	32.4636	0.965626	0.0005
	L2			74		11.5802	0.0017	11.5586	31.7153	0.998145	0.0006
	L3			78		11.7087	0.0020	11.5678	31.7469	0.987968	0.0009
	Pyroxene 1 R Frantz 0.5A + 0xides	0.318	194		11.6124	11.6083	0.0074	11.5259	31.5522	0.992898	0.0028
	L1			77		11.9335	0.0013	11.6096	32.2380	0.972884	0.0005
	L2			197		12.3297	0.0033	11.6338	32.7505	0.943556	0.0007
	Pyroxene 2 R Frantz 0.2A	0.406	45		11.6067	11.5927	0.0246	11.5466	31.6271	0.996019	0.0094
	L1			29		11.9815	0.0037	11.6425	32.2838	0.971742	0.0009
	L2			63		12.4585	0.0044	11.6488	32.8021	0.934958	0.0008
	Pyroxene 3 R Frantz 0.2A hand picked	0.302	15		11.6549	11.5966	0.1025	11.6425	31.6634	1.003956	0.0411
	L1			7		11.9587	0.0071	11.6947	32.2133	0.977963	0.0019
	L2			23		12.1077	0.0045	11.6598	32.3941	0.962975	0.0009
MIL 03346, 175[f]	Whole-rock R	0.249	138		13.0565	13.0505	0.0105	11.7551	32.9319	0.900743	0.0018
	L1			74		13.0453	0.0043	11.7579	34.0813	0.901268	0.0009
	L2			75		12.4076	0.0011	11.6722	32.7221	0.940744	0.0006
	L3			63		12.4107	0.0018	11.6685	32.7225	0.940198	0.0007
	Pyroxene + Olivine R Frantz 0.25A	0.092	56		12.2086	12.2064	0.0332	11.6211	32.4046	0.952048	0.0201
	L2			23		12.9997	0.0060	11.7247	33.3282	0.901920	0.0018
	L3			1		14.4190	0.0674	11.9040	33.9372	0.825577	0.0120
	Pyroxene + Olivine R Frantz 0.10A, d>3.25	0.144	39		11.7728	11.7708	0.0144	11.6627	31.9187	0.990817	0.0044
	L2			9		12.5370	0.0121	11.6992	32.8197	0.933179	0.0026
	L3			2		12.9217	0.0446	11.7568	33.0382	0.909848	0.0055
Chassignite											
Chassigny[j]	Whole-rock R	0.708	10		11.5593	11.5550	0.0230	11.1921	30.6448	0.968594	0.0050
	L1			96		15.1769	0.0019	13.5770	35.4124	0.894572	0.0008
	L2			11		13.3222	0.0073	12.3416	33.6047	0.926428	0.0023
	L3			7		13.4005	0.0059	12.3849	33.6505	0.924221	0.0014

Table 1 (*continued*)

Meteorite name and chemical group	Sample and fraction	Residue weight (g)	Pb[a] (ppb)	Pb (ng)	Uncorr.[b] $^{206}Pb/^{204}Pb$	Corr.[c] $^{206}Pb/^{204}Pb$	Corr.[c] 2σ % err.	Corr.[c] $^{207}Pb/^{204}Pb$	Corr.[c] $^{208}Pb/^{204}Pb$	Corr.[c] $^{207}Pb/^{206}Pb$	Corr.[c] 2σ % err.
Orthopyroxenite											
ALH 84001, 398[f]	Whole-rock R	0.108[d]		0.2	60.2921	61.6845	1.069	36.0689	44.5359	0.58473	0.1822
	L1			2.1	32.0000	32.0228	0.0572	21.6591	50.1455	0.67636	0.0117
	L2			0.9	29.5894	29.6305	0.1422	20.8740	39.7290	0.70448	0.0211
	L3			0.3	65.8973	66.9689	0.7204	37.7883	50.7510	0.56427	0.1276
	L4			1.5	77.0509	77.2993	0.1579	42.4441	51.9875	0.54909	0.0226
	Orthopyroxene R	0.501[d]		2.6	73.7096	73.8421	0.0755	41.0913	57.7196	0.55648	0.0132
	L1			0.7	35.9883	36.0815	0.1610	23.5158	43.3116	0.65174	0.0374
	L2			1.4	32.2012	32.2329	0.0711	22.0570	39.6811	0.68430	0.0157
	L3			1.0	62.7987	63.0738	0.2262	35.9958	53.7553	0.57069	0.0356
	L4			1.5	76.2076	76.4336	0.1477	41.9919	61.0981	0.54939	0.0212
	L5			1.8	65.3826	65.5480	0.1189	37.3806	53.7454	0.57028	0.0199
	d<3.25										
	L2			0.4	26.8552	26.9440	0.3812	19.5790	40.5165	0.72665	0.0577
	L3			0.1	37.3920	38.1393	1.052	24.5824	45.6905	0.64454	0.2437

R = residue after leaching. L# = leachate, # refers to the leaching step.

[a] Pb concentrations estimated from the sample weight and total Pb ion beam signal during mass spectrometric analysis.

[b] Pb isotopic compositions measured by the Lyon MC-ICP-MS (Nu Plasma HR, Nu Instruments) using a DSN-100 desolvating nebulizer. Pb isotope ratios were corrected for mass bias by the Tl doping and standard bracketing method (see text for details).

[c] Uncertainties reported on Pb measured isotope ratios are $2\sigma/\sqrt{n}$ analytical errors in %, where n is the number of measured isotopic ratios. Blank isotope compositions were measured by mass spectrometry ($^{206}Pb/^{204}Pb = 17.80 \pm 0.14$, $^{207}Pb/^{204}Pb = 15.33 \pm 0.13$, $^{208}Pb/^{204}Pb = 37.30 \pm 0.30$, and $^{207}Pb/^{206}Pb = 0.8625 \pm 7$) and corrections were applied to the Pb isotope ratios. Correlated errors due to blank correction are given when applied (see calculations in Bouvier et al., 2007).

[d] Weight before leaching.

[e] P. Gillet (Ecole Normale Supérieure de Lyon) and the Consortium Théodore Monod of the Centre National d'Etudes Spatiales.

[f] US Antarctic Search for Meteorites Program.

[g] J.-A. Barrat (Université de Bretagne).

[h] G. Hupé's private collection.

[i] National Institute for Polar Research.

[j] Muséum National d'Histoire Naturelle in Paris.

An additional enigma adding to the confusion about the current state of the Martian mantle comes from the range in ^{142}Nd and ^{182}W isotopic abundances observed among SNCs, which requires that these magmatic rocks, or at least their sources, formed while the parent nuclides ^{146}Sm ($T_{1/2} = \sim 103$ Ma) and ^{182}Hf ($T_{1/2} = \sim 9$ Ma) were still extant (i.e., during the very early stages of the planet's formation). While ^{146}Sm–^{142}Nd systematics reflect silicate differentiation processes only, ^{182}Hf–^{182}W systematics record both core formation and mantle differentiation events. Therefore, a young age of SNCs associated with ^{142}Nd and ^{182}W anomalies imposes the conclusion that the Martian mantle, which is the most likely source of the SNCs, was not well mixed at the time the SNCs formed (Foley et al., 2005). Elkins-Tanton et al. (2005) suggested that such lack of mixing reflects a mantle stratified with respect to density and, hence, non-convective.

This work presents new Pb isotope data for whole-rocks and mineral separates of eight Martian meteorites including four basaltic, olivine-phyric, lherzolitic and olivine-pyroxene shergottites, two nakhlites, the dunite Chassigny, and the orthopyroxenite Allan Hills 84001. The Pb–Pb chronometer offers the unique advantage that, except for phosphate, ages do not depend on measured parent/daughter ratios and, therefore, are nearly insensitive to recent perturbations. We examine the old ages obtained here within the framework of previously published isotope data on SNCs and use the resulting new chronology to reassess the ^{142}Nd and ^{182}W anomalies found in these meteorites (Kleine et al., 2004; Foley et al., 2005; Debaille et al., 2007; Caro et al., 2008). Mars will be shown to be very similar to the Moon, a planet that due to the LHB went through major resurfacing at 3.9 Ga, but for most of its internal activity otherwise declined some 3.2 to 3.5 Ga ago. As opposed to the Moon, however, Mars experienced a local surge of internal activity at 1.3 Ga, an event attested to by nakhlites and chassignites.

2. Samples and methods

The samples analyzed here are either new finds or Martian meteorite groups that were not previously addressed by Bouvier et al. (2005, 2008a) and, hence, complement these previous studies. Mainly on the basis of variable Sm/Nd ratios, Debaille et al. (2007) recognized three well-defined groups of shergottites, enriched, intermediate, and depleted, which are only loosely related to their petrographic groups (i.e., basaltic, lherzolitic, olivine-phyric). Our new measurements include (a) whole-rocks and maskelynite (the vitreous form of shocked plagioclase) and pyroxene separates of the enriched basaltic shergottite Northwest Africa (NWA) 480 and the enriched lherzolitic shergottite Roberts Massif (RBT) 04262; (b) whole-rocks of the intermediate olivine-phyric shergottite NWA 1068, the depleted olivine-orthopyroxene shergottite NWA 1195, and the chassignite Chassigny; (c) whole-rocks and pyroxene separates of the nakhlites Yamato Mountains (Y-) 000593 and Miller Range (MIL) 03346, as well as the orthopyroxenite Allan Hills (ALH) 84001.

We used the same overall mineral separation and analytical techniques as described previously in Bouvier et al. (2005, 2008a). A few variations introduced to the leaching and dissolution methods are given here. The whole-rock samples dedicated exclusively to Pb isotope work were leached in 1.5 M HBr, 4 M HF, and 2.5 M HCl in ultrasonic bath for 5, 15, and 25 min, respectively. Mineral separates (63–150 μm) for NWA 480 (maskelynite and pyroxene) and Y-000593 (pyroxene) were leached using steps of 4 M HF and 2.5 M HCl (15 min, in ultrasonic bath) and then spiked for Lu–Hf and Sm–Nd isotope work on these same fractions due to the limited amount of mineral separates available. The mineral separates of RBT 04262 and MIL 03346 (63–150 μm) were dedicated to Pb isotope work only and were successively leached in 1.5 M HBr (60 °C, 1 h), 1 M HF (60 °C, overnight), and 6 M HCl (60 °C, 4 h) and only the two last leaching steps were analyzed for their Pb isotopic compositions. An ~0.8 g sample of the orthopyroxenite ALH 84001 was processed to obtain the Pb isotopic composition of the whole-rock and silicate separates, which hence differs from the earlier Pb–Pb study of ALH 84001 carbonates by Borg et al. (1999a). We separated carbonates, maskelynite, and glass from the orthopyroxene on the 63–150 μm fraction (~0.6 g) using heavy liquids (methylene iodine) and hand-picking. We processed the heavy and light fractions separately for

leaching and chemistry. We leached the bulk and mineral separates using a longer protocol than for shergottite and nakhlite separates to first remove terrestrial contamination, and then dissolved progressively the most (carbonates) to least (silicate) soluble phases. The ALH 84001 whole-rock and mineral separates were successively leached in 0.25 M HCl (20 °C, 1 h), 2.5 M HCl (90 °C, 6 h), 6 M HCl (110 °C, 12 h), and 1 M HF (110 °C, 1 h), and finally for the orthopyroxene separates in 4 M HF (110 °C, 16 h). Both leachates and residues of the whole-rock and orthopyroxene separates were analyzed, while only the leachates #2 and #3 were analyzed for the small light fraction. All the residues and leachate solutions were completely dissolved in 0.5 to 20 ml concentrated HF–HNO_3 (5:1), depending on the residue weight (5 to 700 mg). Digestions were done in PFA beakers instead of PTFE bombs to minimize the Pb blank (see Bouvier et al., 2008a). After digestion, samples were processed for element separation and purification following the procedures of Bouvier et al. (2005). The procedures for Pb isotope measurement using the Nu Plasma MC-ICP-MS at ENS-Lyon are described in Bouvier et al. (2008a). Total procedural blanks for the Pb chemistry in general were ~1–5 pg depending on which anlytical protocol was used, but 40 pg for NWA 480 and Y-000593 mineral separates (due to the use of perchloric acid and 7 ml cation-exchange resin beds for Hf and rare earth element (REE) separation prior to final

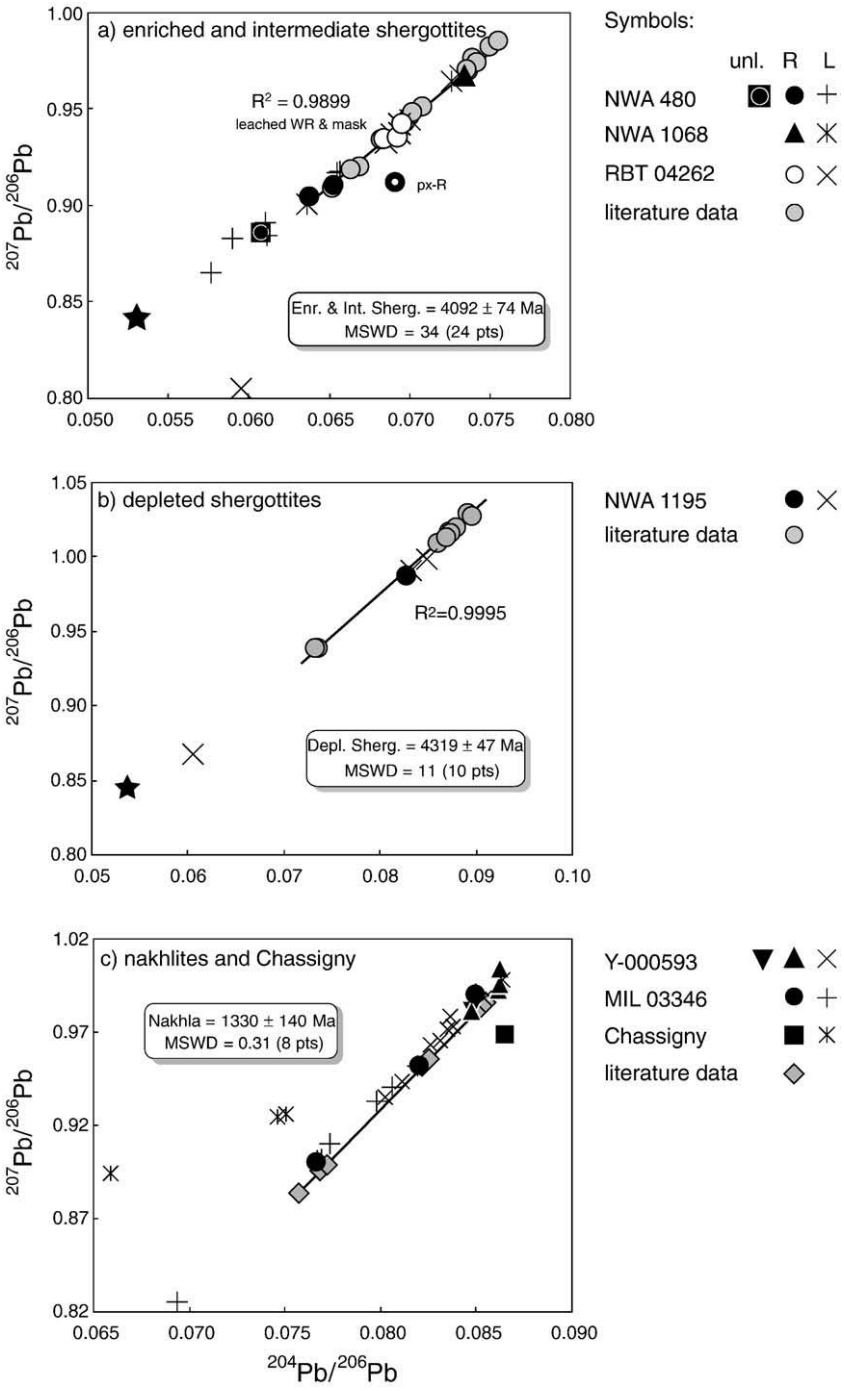

Fig. 1. $^{207}Pb/^{206}Pb$–$^{204}Pb/^{206}Pb$ plots of new Pb isotope data and Pb–Pb ages obtained for residues and leachates of (a) enriched and intermediate NWA 480, NWA 1068, and RBT 04262 compared with literature data on maskelynite and whole-rock residues (Bouvier et al., 2008a and references therein); (b) depleted shergottite NWA 1195 compared with literature data on QUE 94201 (Gaffney et al., 2007); and (c) nakhlites MIL 03346 and Y-000593, and Chassigny compared with literature data on Nakhla (Nakamura et al., 1982; Chen and Wasserburg, 1986b; Bouvier et al., 2005). Star: terrestrial common Pb from Stacey and Kramers (1975). External errors are smaller than symbols.

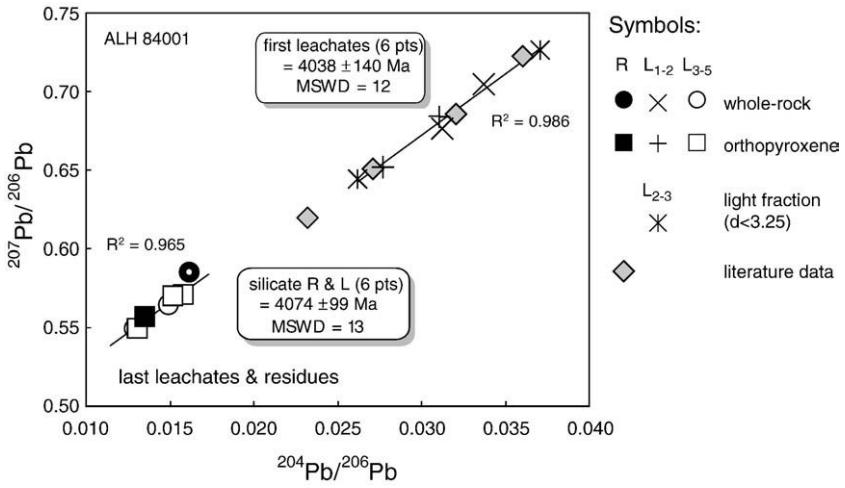

Fig. 2. $^{207}Pb/^{206}Pb$–$^{204}Pb/^{206}Pb$ plot of Pb isotope data of the orthopyroxenite ALH 84001 and Pb–Pb ages obtained for silicate (whole-rock, orthopyroxene, and low-density fractions) residues and leachates (steps L_3, L_4, and L_5) at 4.07 ± 0.10 Ga (MSWD = 12), and first leachate steps (L_1, L_2, and also L_3 of the low-density fraction containing glass, maskelynite, and carbonates) at 4.04 ± 0.14 Ga (MSWD = 12). These isochron ages are concordant with literature data obtained for ALH 84001 obtained by mild leaching, which gave an isochron age for carbonates at 4.04 ± 0.10 Ga (MSWD = 59) (Borg et al., 1999a). External errors are smaller than the symbols.

Pb purification). Therefore, blank corrections for each sample were done according to the corresponding sample/blank ratios. These calculations are detailed in Bouvier et al. (2007). The Lu–Hf and Sm–Nd isotope data obtained simultaneously with the Pb isotope data for some of the samples of this study will be reported elsewhere.

Isotopic compositions of Pb, with Tl used as an internal standard, were measured on the Lyon MC-ICP-MS (Nu Plasma HR, Nu Instruments) using a DSN-100 desolvating nebulizer with an uptake rate of 100 µl/min, resulting in a sensitivity of ~250–300 V/ppm total Pb (Albarède et al., 2004). Typical mean values of $^{206}Pb/^{204}Pb$, $^{207}Pb/^{204}Pb$, $^{208}Pb/^{204}Pb$, and $^{207}Pb/^{206}Pb$ ($2\sigma_m$, $n = 15$) for NBS 981 30 ppb Pb–10 ppb Tl solutions were, respectively, 16.9286 ± 0.0010, 15.4822 ± 0.0009, 36.6664 ± 0.0029, and 0.914558 ± 0.000009. Mean values ($2\sigma_m$, $n = 13$) for 2 ppb Pb–1 ppb Tl NBS 981 solutions were, respectively, 16.930 ± 0.016, 15.485 ± 0.015, 36.675 ± 0.035, and 0.91471 ± 0.00009. The ages presented here were all calculated using Bouvier et al. (2007) for correlations and the Isoplot software of Ludwig (2008).

3. Results

The new Martian meteorite Pb isotope data are listed in Table 1 and plotted in Figs. 1 and 2.

3.1. Enriched and intermediate shergottites

In the 'inverse isochron' plot, $^{207}Pb/^{206}Pb$ vs. $^{204}Pb/^{206}Pb$, the whole-rock and maskelynite residues from NWA 480, NWA 1068, and RBT 04262 (Fig. 1a) fall on the array defined by the corresponding fractions of Zagami (Chen and Wasserburg, 1986a; Borg et al., 2005; Bouvier et al., 2005), Shergotty, and Los Angeles (Bouvier et al., 2008a) and by the intermediate shergottite EETA 79001(Chen and Wasserburg, 1986a). The seven enriched and intermediate shergottites together form an array indicative of an age of 4.09 ± 0.07 Ga (MSWD = 34). Progressive removal of common Pb can be observed for successive leachates (Table 1, and Fig. 1a–c) but, overall, Pb from these samples remains rather unradiogenic (i.e., less radiogenic than common terrestrial Pb). The first steps of leaching and unleached samples show that Antartic meteorites, such as RBT 04262, are less contaminated than hot desert finds, such as NWA 480 (Fig. 1a). The residual maskelynite and whole-rock samples, whether falls or finds, plot on the ~4.1 Ga array, and a two-stage model indicates an average μ_1 value for whole-rocks of ~5.3 (Table 2). The pyroxene residue of NWA 480 is clearly a ternary mixture involving a young Pb component (see Fig. 6 in Bouvier et al., 2008a) attesting to recent disturbance. The whole-rock residue of the olivine-phyric shergottite NWA 1068 is particularly unradiogenic and comparable to Los Angeles (Bouvier et al., 2008a), which suggests that leaching was successful at removing most of the terrestrial and Martian contaminants. The

Table 2
Time-integrated μ_1 ($^{238}U/^{204}Pb$) and μ_1 ($^{147}Sm/^{144}Nd$) values of the enriched, intermediate, and depleted shergottites, nakhlites, Chassigny and ALH 84001 (two-stage evolution), and corresponding crystallization ages T_1 and mean μ_1 values for each group.

Martian meteorites (T_1)	$\mu_1(^{238}U/^{204}Pb)$	$\mu_1(^{147}Sm/^{144}Nd)$
Enriched shergottites (4.1 Ga)		
Zagami	5.2	0.184
Shergotty	5.4	0.183
Los Angeles	5.4	0.178
RBT04262	5.4	–
NWA1068	5.2	–
NWA 480	6.0	–
Average enr. sherg.	5.4	0.182
Intermediate shergottites (4.1 Ga)		
EETA79001	5.2	0.235
ALHA77005	3.6	0.221
LEW88516	6.8	–
Y-793605	5.2	–
Average interm. sherg.	5.2	0.228
Orthopyroxenite (4.1 Ga)		
ALH 84001	~5	0.216
Depleted shergottites (4.3 Ga)		
QUE94201	2.3	0.295
NWA1195	1.8	–
SaU005-008	–	0.295
SaU094	–	0.288
DaG476	–	0.297
Average depl. sherg.	2.0	0.294
Nakhlites (1.3 Ga)		
Nakhla	1.9	0.223
MIL03346	2.1	–
Y-000593/749	1.9	0.231
Governor Valadares	–	0.218
Lafayette	–	0.224
Average nakhlites	1.9	0.224
Chassignite (1.4 Ga)		
Chassigny	1.3	0.206

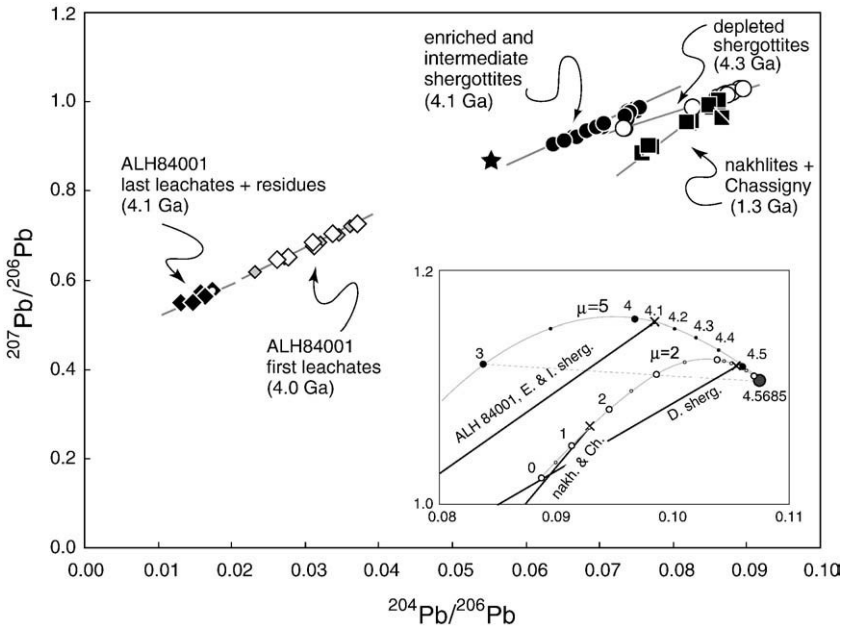

Fig. 3. $^{207}Pb/^{206}Pb$–$^{204}Pb/^{206}Pb$ isochrons of depleted shergottites at ~4.3 Ga, ALH 84001 at ~4.1 Ga, enriched and intermediate shergottites at ~4.1 Ga, and nakhlites and Chassigny at ~1.3 Ga. In this type of plot, ages are given by intercepts with the *y*-axis corresponding to the radiogenic $^{207}Pb^*/^{206}Pb^*$. Data for leached whole-rocks and mineral separates (maskelynite for the shergottites, and pyroxene for the nakhlites and ALH 84001) of Martian meteorites are from this study (Table 1) and the literature (Bouvier et al., 2008a). S4–S7 leachates of the ALH 84001 orthopyroxenite from Borg et al. (1999a) corresponding to a Pb–Pb age of 4.04 ± 0.10 Ga for carbonate formation also are shown (in grey). See also Figs. 1 and 2 for details. Inset: Pb growth curves with different μ_1-values (time-integrated $^{238}U/^{204}Pb$ of the mantle source extrapolated to zero age for the first stage of a two-stage evolution model). The initial Pb isotope composition of the Solar System at 4.5685 Ga is that of the Canyon Diablo Troilite (CDT). The curves are drawn for $\mu_1 = 2$ (representative of the 1.3 Ga old nakhlites and Chassigny, and the 4.3 Ga old depleted shergottites) and $\mu_1 = 5$ (representative of the 4.1 Ga old enriched and intermediate shergottites, and ALH 84001). The μ_1 values calculated for each meteorite are listed in Table 2. Star: terrestrial common Pb from Stacey and Kramers (1975).

large MSWD values, which are a common feature of external isochrons (or, more correctly, errorchrons) for all chronometric systems, show that the data scatter significantly outside of error bars. This may be due to minute amounts of unleached phosphates and oxides and to a range of crystallization ages, which for many of the samples extends over several tens of million years.

3.2. Depleted shergottites

The two last leachates of the whole-rock of the olivine-orthopyroxene shergottite NWA 1195 are less radiogenic ($^{206}Pb/^{204}Pb = 11.77$ and 12.01) than the residue ($^{206}Pb/^{204}Pb = 12.08$) (Table 1, Fig. 1b), which shows that terrestrial contamination is not dominant. This contrasts with DaG 476 (Bouvier et al., 2005), which showed persistence of a terrestrial component in the residue. The whole-rock residue of NWA 1195 falls on the same Pb–Pb array as the mineral phases of the depleted basaltic shergottite QUE 94201 (Gaffney et al., 2007), which, if interpreted as an isochron, collectively gives a Pb–Pb age of 4.32 ± 0.05 Ga (MSWD = 11). NWA 1195 and QUE 94201 have similar trace elements and Sr and Nd isotope characteristics (Symes et al., 2008). In spite of the large MSWD, the Pb–Pb array of depleted shergottites is clearly distinct from the ~4.1 Ga array of enriched and intermediate shergottites (Fig. 3). In addition, the inferred μ_1 of ~2 is conspicuously low, much lower than the value for the enriched and intermediate samples.

3.3. Nakhlites

The Pb–Pb isotope data for whole-rock and pyroxene residues of the nakhlites Y-000593 and MIL 03346 (Fig. 1c) fall on the 1.33 ± 0.14 Ga (MSWD = 0.31) Pb–Pb mineral isochron obtained for Nakhla (Nakamura et al., 1982; Chen and Wasserburg, 1986b; Bouvier et al., 2008a). The μ_1 of ~2 is similar to the value of depleted shergottites (Table 2). The Pb isotopic compositions of the residues plot distinctly off the two shergottite arrays. All the leachates of the whole-rock and pyroxene separates of Y-000593 and MIL 03346 fall on, or slightly off, the ~1.3 Ga reference internal isochron of Nakhla attesting to a lesser contamination of these two Antarctic meteorites with respect to a hot desert find such as NWA 998 (Carlson and Irving, 2004). Lead in the pyroxene residue is less radiogenic than Pb in the whole-rock residues and the leachates, which points to phosphates as a major U carrier. This emphasizes the well-known difficulty of dating ultramafic rocks, such as dunites and clinopyroxenites, in which Pb and U are not hosted by a major mineral phase (Fig. 1c).

3.4. Chassigny

This fall, which was dated at ~1.39 Ga by different chronometers, comes from a mantle source different from that of Nakhla and Y-000593 (Misawa et al., 2006). Lead isotopes in three successive leachates of the whole-rock of Chassigny suggest the presence of a component with a composition similar to that of terrestrial common Pb, but nevertheless the residue falls close to the ~1.3 Ga Nakhlite errorchron (Figs. 1c and 3).

3.5. The orthopyroxenite ALH 84001

This sample presents the most radiogenic Pb isotopic composition among Martian meteorites (Fig. 2 and Table 1). The leachates and residues of the whole-rock and mineral separates define a distinctive Pb–Pb alignment. The first two leachates of the whole-rock and of the orthopyroxene separates, and the second and third leachates of the low-density phase, have $^{206}Pb/^{204}Pb$ ratios consistent with the data of Borg et al. (1999a). They define an array indicative of an age of 4038 ± 140 Ma (MSWD = 12). The following, stronger, leachates of the whole-rock (L_3 and L_4) and orthopyroxene separates (L_3, L_4 and L_5) are even more radiogenic, while the residues show the most radiogenic Pb isotope compositions measured so far for Martian meteorites. The whole-rock residue contains less than 0.2 ng of Pb (Table 1) and, due to the large error associated with this isotope measurement, was excluded from the Pb–Pb age calculations. Together, the strong leachates (L_3 to L_5) and the orthopyroxene residue define an array with an age of 4074 ± 99 Ma

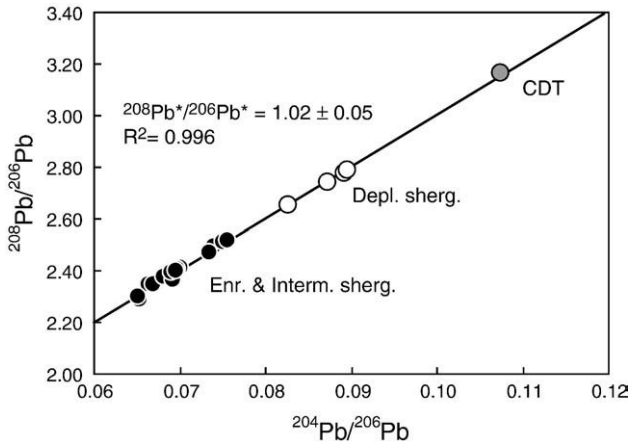

Fig. 4. Estimate of the Th/U ratio of shergottites from their range of $^{208}Pb/^{206}Pb$. Initial $^{208}Pb^*/^{206}Pb^* = 1.02 \pm 0.05$ for the enriched, intermediate, and depleted shergottites (Pb–Pb isotope data of leached whole-rocks and maskelynite separates from this study and the literature (Bouvier et al., 2005, 2008a)). The Canyon Diablo Troilite (Tatsumoto et al., 1973) composition falls on the isochron, hence attesting to little Th/U fractionation during Mars accretion and differentiation or during extraction of shergottite magmas. The Th/U ratio inferred for Mars is 3.9 for 4.1 Ga old shergottites (in agreement with its value for the Sun, carbonaceous chondrites, and the Earth), but decreases to 3.2 if shergottites are <0.5 Ga old (see Fig. 5).

(MSWD = 11) indistinguishable from each of the arrays defined by the first leachates, by the leachate analyses of Borg et al. (1999a), and by the enriched and intermediate shergottites. The radiogenic composition of the first leaching steps attests to minimal contamination by common Pb.

3.6. $^{208}Pb/^{206}Pb$ variability

All shergottites define a single array in the $^{208}Pb/^{206}Pb$ vs. $^{204}Pb/^{206}Pb$ diagram, which gives an initial $^{208}Pb^*/^{206}Pb^* = 1.02 \pm 0.05$ (Fig. 4). For the pyroxene and whole-rock residues of the three nakhlites, the initial $^{208}Pb^*/^{206}Pb^*$ value is 1.24 ± 0.24. In contrast, $^{208}Pb/^{206}Pb$ of the leachates and residues of ALH 84001 shows a common trend with $^{208}Pb^*/^{206}Pb^* = 0.31 \pm 0.10$.

4. Discussion

The most important results of the present work hinge around (a) the two groups of Pb–Pb ages obtained for enriched and intermediate shergottites and ALH 84001 at ~4.1 Ga, and for depleted shergottites at ~4.3 Ga, which provides a simple chronology consistent with cratering evidence, and (b) the confirmation of the 1.3 Ga age of nakhlites, which discounts contamination of SNCs by terrestrial Pb. To assist the discussion of these results and their implications for the early history of Mars, we will explain (i) why whole-rock Pb–Pb variability cannot be accounted for by mixing arrays, (ii) present new evidence that the $^{208}Pb/^{206}Pb$ data do not support young emplacement ages, and (iii) provide a re-interpretation of extinct radioactivity evidence in accordance with the perspective of old shergottite ages.

4.1. The age of ALH 84001

As attested to by its ~15 Ma exposure age (Nyquist et al., 2001), ALH 84001 comes from a unique launch event. This sample was believed to be ~4.5 Ga old, on the basis of two independent Sm–Nd mineral isochrons (Jagoutz et al., 1994; Nyquist et al., 1995), while the ~4.0 Ga ages obtained from Rb–Sr and Ar–Ar data were interpreted as reflecting a later shock event (Nyquist et al., 2001 and references therein). Rb–Sr and Pb–Pb ages of ~4.0 Ga have previously been obtained on carbonates and leachates of ALH 84001 (Borg et al., 1999a). ALH 84001 is the only Martian meteorite with Pb more radiogenic than common terrestrial Pb. We found that the ages of the Pb–Pb silicate mineral (whole-rock and orthopyroxene) and leachate isochrons at, respectively, 4074 ± 99 Ma (MSWD = 11) and 4038 ± 140 Ma (MSWD = 12), are not significantly different. This makes ALH 84001 of the same crystallization age as the enriched and intermediate shergottites (Fig. 3) and leaves the depleted shergottites as the oldest Martian meteorites.

4.2. Whole-rock isotopic data, mixing, and evidence against terrestrial contamination

The large spread of present-day isotope compositions observed in shergottites for $^{87}Sr/^{86}Sr$ (0.701–0.721), $^{143}Nd/^{144}Nd$ (0.5125–0.5159), and $^{176}Hf/^{177}Hf$ (0.2822–0.2842) clearly requires billions of years of evolution in isolated reservoirs. The persistence of a linear array of whole-rocks in the $^{87}Sr/^{86}Sr$ vs. $^{87}Rb/^{86}Sr$ plot with an age older than 4.0 Ga is remarkable but, on account of the young ages of mineral isochrons, the old age given by this whole-rock array has commonly been dismissed and instead been interpreted as a mixing line. The case of magma mixing has been addressed elsewhere (Bouvier et al., 2008a).

Bouvier et al. (2008a) also made the case that their Pb–Pb isochrons, on which plot leached whole-rock and maskelynite from different samples, could not result from contamination by terrestrial Pb (as argued by, for example, Gaffney et al., 2007), because 3-component mixtures of a terrestrial contaminant, common Martian Pb, and radiogenic Pb are not expected to form linear arrays in binary plots involving two Pb isotope ratios. Intersection of the two shergottite arrays and ALH 84001 in one point requires a different clarification. Stacey and Kramers (1975) demonstrated that six terrestrial isochrons converge toward one point: for a two-stage evolution, the point on which secondary isochrons intersect represents the mean isotope composition of the common reservoir and lies on the planetary primary isochron (geochron). The same common intercept also was found for another 20 terrestrial isochrons (Manhès et al., 1979). Martian shergottites are not more 'contaminated' by terrestrial common Pb than samples of terrestrial isochrons. Therefore, appealing to massive, yet elusive, contamination of Martian samples by terrestrial Pb is, with the exception of some desert finds such as the nakhlite NWA 998 (Carlson and Irving, 2004) and the olivine-orthopyroxene shergottite DaG 476 (Bouvier et al., 2005), unnecessary. What the point common to Mars and the Earth does indicate, however, is that the Martian mantle prior to its differentiation into the low-μ source of shergottites (Jagoutz, 1991; Bouvier et al., 2008a) and the high-μ source of ALH 84001 had a mean U/Pb ratio similar to that of the mantle source of the terrestrial continents. The U/Pb evolution of the mantles of both planets thus may have been quite similar.

Mixing is not supported either by the so-called 'mixing plot' such as $^{206}Pb/^{204}Pb$ vs. 1/Pb. First, the available Pb concentration data have been badly affected by leaching. Second, this mixing plot makes the untenable assumption that each member contributes to each mixture with a uniform Pb *concentration*, in contrast to conventional isochron plots that only require uniform isotopic (or elemental) *ratios*. Variable mineral abundances and magmatic differentiation combine to change Pb concentrations and therefore destroy the linear mixing relationship. Anyhow, the scatter of shergottites in the actual $^{206}Pb/^{204}Pb$ vs. 1/Pb plot (not shown) does not support the mixing hypothesis.

Lastly, the present Pb isotope data for whole-rock and pyroxene residues of the nakhlites Y-000593 and MIL 03346 (two finds), and for Chassigny, are concordant with the 1.33 ± 0.14 Ga Pb–Pb internal isochron obtained for Nakhla (Nakamura et al., 1982; Bouvier et al., 2008a). Despite Pb concentrations being significantly lower in nakhlites than in shergottites, the former do not plot on a tie-line going through terrestrial Pb, which unambiguously shows that nakhlites eluded terrestrial contamination. Unless it is assumed that nakhlites by nature are less prone to terrestrial contamination than shergottites or ALH 84001, the nakhlite data, therefore, demonstrate

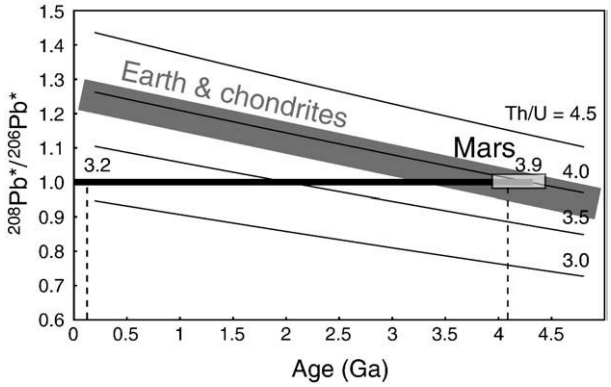

Fig. 5. Evolution of radiogenic $^{208}Pb^*/^{206}Pb^*$ with Th/U and time in planetary systems such as chondrites (Th/U ~ 3.9 ± 0.2; Rocholl and Jochum, 1993), the Earth (Th/U ~ 3.85; Galer and O'Nions, 1985), and Mars. For Mars, the shergottite isochron (Fig. 4) gives $^{208}Pb^*/^{206}Pb^* = 1.02 \pm 0.05$, which implies Th/U of ~3.9 for a crystallization age of 4.1 Ga, in agreement with the Th/U of chondrites and the Earth, but at odds with the ~3.2 value for a crystallization age of 0.2 Ga.

that the crystallization age of all Martian meteorites can be, and has been, obtained accurately by Pb–Pb chronometry.

4.3. Th–U evidence of old shergottite ages

Further evidence for old shergottites is provided by the ratio of radiogenic $^{208}Pb^*$ to $^{206}Pb^*$ of 1.02 ± 0.05 deduced from the intercept of the $^{208}Pb/^{206}Pb$ vs. $^{204}Pb/^{206}Pb$ alignment (Fig. 4) in precisely the same way as $^{207}Pb^*/^{206}Pb^*$ is calculated from the "inverse" isochron plot. This ratio corresponds to a modern Th/U ratio of ~3.9 for 4.1–4.3 Ga old shergottites, and to ~3.2 if they are <0.5 Ga old (Fig. 5). The Th/U values are inferred for the *last stage* of radiogenic ingrowth and do not depend significantly on the recent history (<0.5 Ga) of the samples (Fig. 5). The Th/U ratio found for an age of 4.1–4.3 Ga for the shergottites is indistinguishable from the Th/U ratio of 3.9 ± 0.2 found for the Earth, the Sun, and carbonaceous chondrites (Galer and O'Nions, 1985), and also from the time-integrated Th/U ratio derived from the Pb isotope compositions of most lunar rocks (Tera and Wasserburg, 1975). The fractionation of Th from U, two highly refractory elements, being very unlikely during accretion (Fig. 4), $^{208}Pb/^{206}Pb$ provides additional evidence for old shergottites. The nakhlite $^{208}Pb^*/^{206}Pb^*$ value of 1.24 ± 0.24 at ~1.3 Ga is too imprecise to be useful. The low value of $^{208}Pb^*/^{206}Pb^*$ for ALH 84001 reflects orthopyroxene/melt fractionation with $D_{Th} \approx 0.4\ D_U$ (Blundy and Wood, 2003).

4.4. Two groups of old emplacement ages

The pattern of shergottite ages is reminiscent of that of shocked eucrites, in which internal Rb–Sr, Sm–Nd, and Pb–Pb isochrons, as well as Ar–Ar ages, commonly have been reset by impacts (Tera et al., 1997). Such isochron rotations and Ar resetting have been reproduced in reheating experiments (Nyquist et al., 1991). The case for old shergottites is not truly novel (Bogard et al., 1979) but has been dismissed mostly on the basis of concordance among younger ages from phosphate-hosted chronometers (e.g., U–Pb, Sm–Nd). Borg et al. (1999b) argued that the lack of textural evidence of reheating (Jones, 1986) does not rule out resetting of Ar–Ar, Rb–Sr, and Sm–Nd internal isochrons. Bouvier et al. (2008a) emphasized that the Pb isotope data of whole-rock and the Pb-hosting silicate phase maskelynite of basaltic, olivine-phyric, and lherzolitic shergottites fall on the same linear array with an age of 4.1 ± 0.1 Ga (Figs. 1a and 2). The new Pb isotope data of whole-rock and mineral residues of the shergottites NWA 480, NWA 1068, and RBT 04262 presented here (Table 1) fall on the ~4.1 Ga old array of Bouvier et al. (2008a) as does the more radiogenic ALH 84001, while the whole-rock residue for the olivine-orthopyroxene shergottite NWA 1195 (Table 1) falls on the 4.33 ± 0.02 Ga internal Pb–Pb errorchron of the depleted basaltic shergottite QUE 94201 (Gaffney et al., 2007). There is no issue about the post-resetting evolution of the Pb isotope composition because not enough time is allowed for radiogenic ingrowth: Pb–Pb in shergottites reproduces the same apparent chronological paradox as the Wyoming and other granites which, although they lost up to 70% of their U over the last tens of Ma, nevertheless preserved in their feldspars the Pb–Pb record of their Archean crystallization (Rosholt and Bartel, 1969).

Consequently, the young ages (180–575 Ma) obtained for shergottites by ^{87}Rb–^{87}Sr, ^{147}Sm–^{143}Nd, ^{176}Lu–^{176}Hf, and U–Pb mineral isochrons must reflect resetting of these chronometers by either strong impacts or fluid percolation on length scales commensurate with mineral grain size and do not date the crystallization of the magmas themselves (Bouvier et al., 2008a). Incipient re-equilibration is caught in the act in NWA 2737, a shocked chassignite with a 1.39 Ga Sm–Nd age (Misawa et al., 2005, 2006) and yet having an Ar–Ar age of 165 Ma (Bogard and Garrison, 2008). Resetting can be explained by the dominant role played by fragile phosphates in Martian meteorites on the overall SNC REE and U budgets (Wadhwa et al., 1994) and by melt inclusions in the minerals, notably pyroxene, used for dating purposes. As discussed by Bouvier et al. (2008a), the similar δD values of phosphates and the Martian atmosphere (Greenwood et al., 2008) suggest interaction of the samples with groundwater. In contrast, the more robust plagioclase hosts a substantial fraction of the rock's Pb, as well as its Sr, thus aiding in preserving the original chronological information carried by these two elements (Bouvier et al., 2005). Furthermore, REE in phosphate readily record fluid circulation

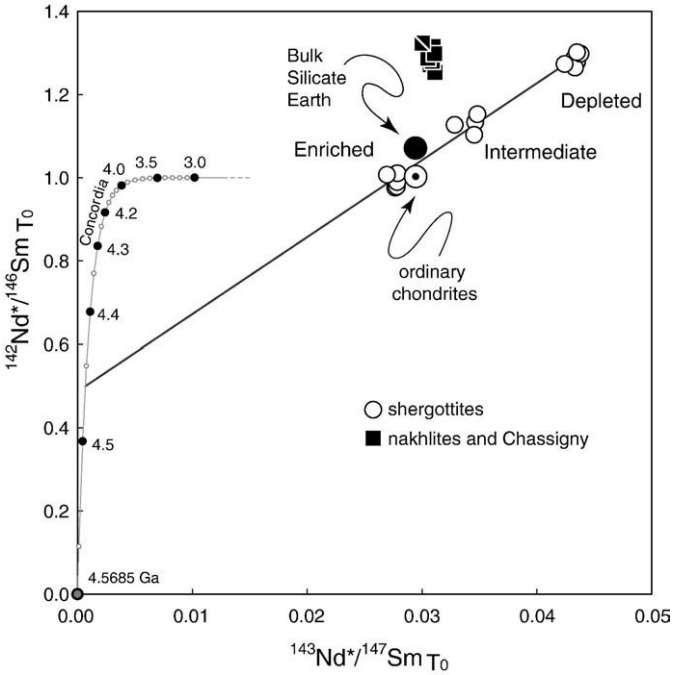

Fig. 6. $^{142}Nd^*/^{146}Sm_{T0}$–$^{143}Nd^*/^{147}Sm_{T0}$ Concordia for enriched, intermediate, and depleted shergottites, as well as nakhlites and Chassigny (Sm–Nd isotopic data from Debaille et al., 2007, and Caro et al., 2008, excluding NWA 1183 and Dhofar 019). The symbol * refers to the radiogenic Nd isotopes accumulated since T_0, the age of the Solar System (see equations in Appendix A). The black square with the white cross bar represents Chassigny. The unfractionated reservoir with the $^{143}Nd/^{144}Nd$ and $^{142}Nd/^{144}Nd$ ratios of ordinary chondrites (Boyet and Carlson, 2005; Bouvier et al., 2008b) plots on the Concordia at $T = 0$. A point that lost all its Sm at T' would plot on the Concordia at that age. The lines going through the points of these rocks and of ordinary chondrites indicate late crystallization of the magma ocean or a giant impact at ~4.47 Ga. Nakhlites clearly plot above this line because of the strong Sm/Nd fractionation between the melts and their mantle source (Longhi, 1991; Borg et al., 2003).

(Lecuyer et al., 2004), hence rendering the Sm–Nd system more susceptible to disturbance than the Rb–Sr system.

4.5. Implications of the revised older age for the differentiation of Mars

The observation that chondrite ε_{142Nd} and ε_{143Nd} plot slightly off the shergottite array combined with the assumption that shergottites are young led Debaille et al. (2007) to infer that this array is indicative of mixed sources. However, Caro et al. (2008) explained the same observations by concluding that Mars has a non-chondritic Sm/Nd ratio. At this stage in the debate, the Nd isotope data on SNCs therefore receive the two alternative, and possibly irresolvable, interpretations of whether the data reflect a multistage magmatic history or whether Mars inherited a non-chondritic Sm/Nd ratio. An important aspect of this debate was alluded to above: a very substantial fraction of the Nd is hosted in phosphates and not in silicate minerals. Moreover, all the ε_{142Nd} and ε_{143Nd} data on shergottites involve unleached samples.

A comprehensive perspective on the petrogenetic relationships between the different SNCs, including fractionation of the parent/daughter ratios, can be obtained from a $^{142}Nd^*/^{146}Nd_{T0}$ vs. $^{143}Nd^*/^{147}Sm_{T0}$ Concordia plot (Fig. 6), conceptually similar to Wetherill's U–Pb Concordia, where the * symbol refers to all the radiogenic Nd produced by radioactivity since the formation of the Solar System and T_0 refers to the age of the Solar System, which is taken as 4.5685 Ga (Bouvier et al., 2007). The Concordia maps the trajectory of a point representing unfractionated material from the solar nebula through time. The equations of this Concordia are described in the Appendix A. The most visible feature of the ε_{142Nd}–ε_{143Nd} Concordia is the rapid decay of ^{146}Sm prior to 4.1 Ga (Fig. 6). A sample plotting on the Concordia at 0 would have remained unfractionated for 4.5685 Ga, while a sample plotting at T would have lost all its Sm at that age. The shergottite data form a linear array that intersects the Concordia at 4.47 Ga, which is the age of a major Sm/Nd fractionation event, and may date either the end of magma ocean crystallization or the major impact that is seen as responsible for the crustal dichotomy (e.g., Frey et al., 2002). The source of Sm and Nd in the enriched shergottites was not fractionated, whereas the Sm/Nd ratios in the sources of intermediate and depleted shergottites sharply increased at 4.47 Ga, which is in agreement with the Sm/Nd ratios of these samples (Debaille et al., 2007). Clearly, the Sm/Nd ratios, if of magmatic origin, were not appreciably changed by melting at 4.1 or 4.3 Ga: this should not necessarily be seen as an issue since Sm/Nd fractionation during MORB melting hardly exceeds 5–10%, which is a very small change on the scale of Fig. 6. Shergottites were therefore produced by large degrees of melting with olivine and orthopyroxene dominating the residues. The rock Sm/Nd ratios hence reflect, to a good approximation, the value of the source, which previous studies have likened to pyroxene-rich cumulates from the magma ocean (Wadhwa et al., 1994; Borg et al., 2003). Alternatively, if Sm and Nd are hosted essentially by first-order phosphate, the array of Fig. 6 may be seen as a mixing line between old but labile components with Sm and Nd redistribution taking place during the young (e.g., 180 Ma old) resetting event. Not enough time was left anyway after the perturbation for substantial scatter to develop in Fig. 6.

Two-stage models of Sm–Nd and U–Pb evolution were calculated for each sample assuming that they formed at time T_1, which is either at 4.1 Ga (for the enriched and intermediate shergottites) or 4.3 Ga (for the depleted shergottites) and at 1.3 Ga (for the nakhlite–Chassigny group). The customary symbol μ is used to refer to the parent–daughter ratios extrapolated to the present day, except for $\mu(^{146}Sm/^{144}Nd)$, which is extrapolated to T_0. Although this model is oversimplified, it nevertheless provides a useful first-order estimate of the parent–daughter ratio (μ_1) of the different systems integrated over the pre-eruption period. The results are shown in the inset of Fig. 3 for the combined U–Pb systems, and the calculated μ_1 values for the U–Pb and ^{147}Sm–^{143}Nd systems are listed in Table 2. The full set of equations is given in Appendix A. As previously discussed by Jagoutz (1991), low values of μ_1 ($^{238}U/^{204}Pb$) are obtained for enriched (e.g., Shergotty) and intermediate (e.g., EETA 79001) shergottites, and ALH 84001 (~5), depleted shergottites (typified by QUE 94201 and NWA 1195; ~2), and nakhlites (e.g., Nakhla; ~2). Depleted shergottites have the highest $\mu_1(^{147}Sm/^{144}Nd)$ values, which point to a light-REE depleted source, presumably pyroxene cumulates in agreement with inferences from ε_{142Nd}–ε_{143Nd} systematics. As expected, the enriched shergottites have the lowest *and* near-chondritic $\mu_1(^{147}Sm/^{144}Nd)$ values. The most straightforward interpretation of these results and ^{142}Nd evidence is that depleted shergottites formed from early pyroxene cumulates of the Martian magma ocean (high Sm/Nd and low U/Pb), while enriched shergottites formed later, after convection had begun to mix the residual liquids, as well as the uppermost layers they crystallized from, back into the deep cumulates, thereby bringing trace element abundances back to near-

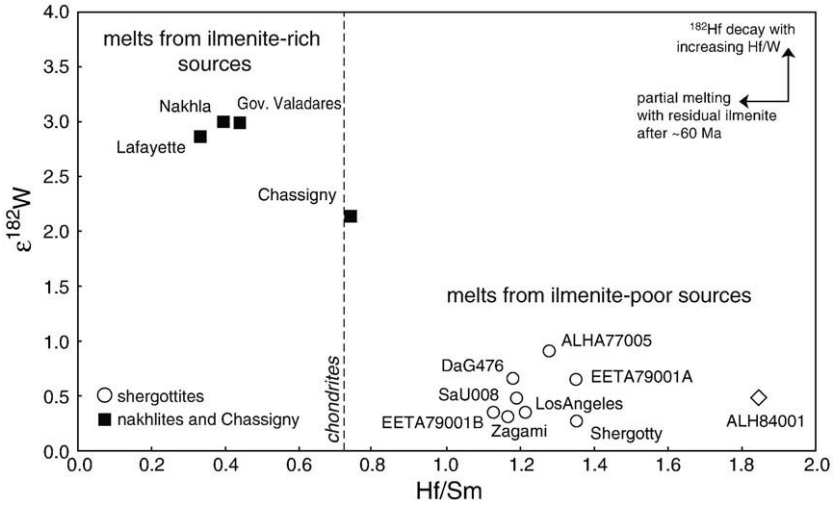

Fig. 7. Correlation between ε^{182}W and Hf/Sm for Martian meteorites. This ratio is particularly insensitive to mineral fractionation in planetary basalts until ilmenite saturation is reached. The dashed line represents the chondritic value for Hf/Sm = 0.72. The correlation indicates that the process which fractionated ε^{182}W between nakhlites, Chassigny, shergottites, and ALH 84001 (W isotopic data from Kleine et al., and Foley et al.,) is probably the same as that which fractionated Hf from Sm. The arrows in the upper right-hand corner show the effect of ^{182}Hf decay (λ_{182Hf} = 8.9 Ma) and partial melting involving ilmenite fractionation on the ^{182}W during the three-stage history of the nakhlites and their mantle source. This plot therefore demonstrates that the mantle source of nakhlites and chassignites formed as ilmenite-bearing cumulates within the first 20 Ma after accretion (Kleine et al., 2004 and Foley et al., 2005), then remained isolated from mantle convection and melted at 1.3 Ga.

chondritic values (Table 2). As on Earth, convection on Mars works at reducing heterogeneity.

In this new scenario, we also reconsider the nature of the source and of the 1.3 Ga event recorded by the rare nakhlites and the even rarer chassignites. Nakhlites are highly enriched in very incompatible elements, yet their initial $^{143}Nd/^{144}Nd$ is very radiogenic (Nakamura et al., 1982), which designates these rocks as small-degree melts of a depleted source (Borg et al., 2003). Nakhlites and Chassigny show large excesses of ^{182}W ($\varepsilon^{182}W \approx 2$–3) compared to shergottites and ALH 84001 ($\varepsilon^{182}W \approx 0.5$) suggesting that the source of nakhlites separated less than 20 Ma after the planet formed (Kleine et al., 2004), i.e., shortly before the source of shergottites. Just as lunar high-Ti basalts (Taylor and Jakes, 1974), the ^{182}W abundances in nakhlites can be explained by the melting at 1.3 Ga of ilmenite-rich cumulates (Righter and Shearer, 2003). A compelling indication in favor of this proposition is the strong negative correlation observed between $\varepsilon^{182}W$ and Hf/Sm ratios (Fig. 7). The Hf/Sm ratio is known to be particularly insensitive to the fractionation of basaltic minerals until very late in the fractionation path, when ilmenite finally begins to precipitate (Blichert-Toft et al., 1999). The Hf/Sm ratio in shergottites and ALH 84001 is higher than the chondritic value (0.72; Bouvier et al., 2008a,b), whereas it is lower in nakhlites (Blichert-Toft et al., 1999). We consider that the mineralogy of the Martian upper mantle consists of cumulates from the magma ocean. Ilmenite is the only common phase that can withhold Hf in the source of nakhlites much more efficiently than Sm. Such scattered ilmenite-rich cumulates, therefore, had to have formed less than 20 Ma after accretion and then quickly sank into the mantle because of the large specific gravity of this mineral relative to its surroundings. The Hf/Sm data of SNCs combined with the corresponding ^{182}W anomalies are consistent with nakhlites representing melts from late-stage cumulates with residual ilmenite, whereas shergottites are melts of ilmenite-poor cumulates. The eruption of nakhlites at 1.3 Ga thus represents an isolated event of melting due to the convective upwelling of a mantle domain of particular composition and not a renewed surge in global planetary magmatic activity.

4.6. A new chronological framework for the evolution of the interior of Mars

From the above discussion emerges that a gravitationally stable layered mantle on Mars (Foley et al., 2005) is no longer demanded by the geochemical observations. Our new chronological framework permits most of the Martian mantle activity to be restricted to pre-LHB time. The first few hundreds of Ma witnessed first the crystallization of the magma ocean, which resulted in a strongly layered mantle, then the subsequent homogenization of the mantle source of shergottites by convection. The mantle was still hot enough to sustain strong volcanic activity for the first 500 My. Shergottites and ALH 84001 represent samples of the upper and the middle crust formed before or during the LHB. The ~4.0 Ga (Pb–Pb) old carbonates of ALH 84001 (Figs. 2 and 3), together with interstitial silica and sulfides, represent hydrothermal activity associated with the last gasps of shergottitic magmatism. Extensive surface melting by the LHB could have brought plate tectonics on Mars to its end and with that the demise of its magnetic field as reflected by the formation of large demagnetized Martian basins as early as ~4.0 Ga or even earlier (Werner, 2008). In contrast, nakhlites and chassignites may represent the infilling by the major volcanoes of Tharsis or Syrtys Major, or the wide craters left by the LHB, in much the same way as lunar mare basalts represent the infilling of impact craters on the Moon. The rarity of Martian surface with the appropriate age to account for young shergottites would no longer be an issue. The present interpretation thus recasts all the multi-chronometric data on all the different Martian meteorite types into a time frame consistent with cratering rates (Frey, 2006). It also relieves the need for elusive widespread modern volcanic activity and re-establishes Mars as a convecting planet, at least during the first hundreds of million years of its history.

4.7. Implications for the impact history of the Martian surface and the origin of SNC meteorites

In contrast to the young shergottite crystallization ages, which imply that these meteorites were ejected exclusively from calderas or from the rare and thin flows within the Tharsis volcanic area, the new ancient Pb–Pb ages remedy the difficulty of provenance. Old shergottite ages alleviate the need for preferential extraction of coherent material (Hartmann and Barlow, 2006), which clearly does not account for the presence of basalts and regolith among lunar meteorites (Righter, 2008). The oldest Martian meteorites are now represented by the group of depleted shergottites at ~4.3 Ga, which is comparable to the oldest lunar rocks (Sokol et al., 2008) and also to the oldest Martian basin ages (Werner, 2008). This suggests that the pre-4.3 Ga crusts have been obliterated from the surface of terrestrial planets and were reprocessed by intense impacts in the early Solar System.

It seems that each cluster of young mineral isochron ages can be associated with a different ejection age (see Fig. 2 of Fritz et al., 2007), which is best explained by local resetting events. Major break-up events in the asteroid belt have been identified at 160 and 450 Ma (Nesvorny et al., 2005; Bottke et al., 2007). If the shergottite isochron ages date impact events at the surface of Mars, young ages should be ubiquitous on other planets as well, but they are not. We suggest that this is a consequence of the presence of water in the Martian ground (Leshin Watson et al., 1994; Blichert-Toft et al., 1999). The radial morphology of crater ejecta on the Moon demonstrates the dry character of the lunar regolith. On Mars, however, the presence of water in the ground shows up as layered warm or hot ejecta blankets draped around craters (Carr et al., 1977). Water pressurized during impacts increased the efficiency of resetting, notably of phosphate and glasses (see a discussion of the effect of sub-surface volatiles in Barlow, 2008). As suggested by Bouvier et al. (2005), the young isochron ages may also reflect the last dry-out of local low-pH lakes (Fairen et al., 2004) or aquifers, but these two interpretations may be seen as two end-members of a broader composite model, specific to Mars, in which water plays a dominant role in the resetting of igneous ages.

5. Conclusions

New Pb isotopic data on Martian meteorites favor three groups of formation ages: 4.3 Ga for the depleted shergottites, 4.1 Ga for ALH 84001 and the intermediate and enriched shergottites, and 1.3 Ga for nakhlites and Chassigny. The young ages indicated by Rb–Sr, Sm–Nd, Lu–Hf, and U–Pb internal isochrons of shergottites reflect recent resetting by either fluids or impacts. The role of magma mixing in creating the isotopic patterns of Martian meteorites is minimal. Shergottites and ALH 84001 represent samples all derived from a volcanic basement subsequently shattered by the ~3.9 Ga old LHB. This revised chronology is consistent with cratering rate history and active convection of the Martian mantle. Nakhlites and chassignites correspond to decompression melting of ilmenite-rich mantle domains and not to renewed global magmatic activity of the planet. The history of the interior of Mars, therefore, resembles that of the Moon.

Acknowledgements

We are grateful for the meteorite allocations (Philippe Gillet, Bertrand Van de Moortèle, Jean-Alix Barrat, Consortium Théodore Monod of the Centre National d'Etudes Spatiales, Muséum National d'Histoire Naturelle de Paris, National Institute for Polar Research, and US Antarctic Search Meteorite Program) and the steady financial support from the French Programme National de Planétologie. We likewise acknowledge financial support from the French Agence Nationale de la Recherche. Comments by several anonymous reviewers and the editor Rick Carlson helped improve the manuscript. We are also indebted to Philippe Telouk and Chantal Douchet for their assistance during the mass spectrometry and laboratory work.

Appendix A. Supplementary data

Supplementary data associated with this article can be found, in the online version, at doi:10.1016/j.epsl.2009.01.042.

References

Albarède, F., Télouk, P., Blichert-Toft, J., Boyet, M., Agranier, A., Nelson, B., 2004. Precise and accurate isotopic measurements using multiple-collector ICP-MS. Geochim. Cosmochim. Acta 68, 2725–2744.

Barlow, N.G., 1988. Crater size–frequency distributions and a revised Martian relative chronology. Icarus 75, 285–305.

Barlow, N.G., 2008. Mars: An Introduction to its Interior, Surface and Atmosphere, Eds. Cambridge Planetary Science, 264 p.

Blichert-Toft, J., Gleason, J.D., Télouk, P., Albarède, F., 1999. The Lu–Hf isotope geochemistry of shergottites and the evolution of the Martian mantle–crust system. Earth Planet. Sci. Lett. 173, 25–39.

Blundy, J., Wood, B., 2003. Partitioning of trace elements between crystals and melts. Earth Planet. Sci. Lett. 210, 383–397.

Bogard, D.D., Garrison, D.H., 2008. ^{39}Ar–^{40}Ar age and thermal history of martian dunite NWA 2737. Earth Planet. Sci. Lett. 273, 386–392.

Bogard, D.D., Husain, L., Nyquist, L.E., 1979. ^{40}Ar–^{39}Ar age of the Shergotty achondrite and implications for its post-shock thermal history. Geochim. Cosmochim. Acta 43, 1047–1055.

Borg, L.E., Connelly, J.N., Nyquist, L.E., Shih, C.-Y., Wiesmann, H., Reese, Y., 1999a. The age of the carbonates in Martian meteorite ALH84001. Science 286, 90–94.

Borg, L.E., Norman, M., Nyquist, L.E., Bogard, D.D., Snyder, G.A., Taylor, L.A., Lindstrom, M., 1999b. Isotopic studies of ferroan anorthosite 62236: a young lunar crustal rock from a light rare-earth-element-depleted source. Geochim. Cosmochim. Acta 63, 2679–2691.

Borg, L.E., Nyquist, L.E., Wiesmann, H., Shih, C., Reese, Y., 2003. The age of Dar al Gani 476 and the differentiation history of the martian meteorites inferred from their radiogenic isotope systematics. Geochim. Cosmochim. Acta 67, 3519–3536.

Borg, L.E., Edmunson, J.E., Asmerom, Y., 2005. Constraints on the U–Pb isotopic systematics of Mars inferred from a combined U–Pb, Rb–Sr, and Sm–Nd isotopic study of the Martian meteorite Zagami. Geochim. Cosmochim. Acta 69, 5819–5830.

Bottke, W.F., Vokrouhlicky, D., Nesvorny, D., 2007. An asteroid breakup 160 Myr ago as the probable source of the K/T impactor. Nature 449, 48–53.

Bouvier, A., Blichert-Toft, J., Vervoort, J.D., Albarède, F., 2005. The age of SNC meteorites and the antiquity of the Martian surface. Earth Planet. Sci. Lett. 240, 221–233.

Bouvier, A., Blichert-Toft, J., Moynier, F., Vervoort, J.D., Albarède, F., 2007. Pb–Pb dating constraints on the accretion and cooling history of chondrites. Geochim. Cosmochim. Acta 71, 1583–1604.

Bouvier, A., Blichert-Toft, J., Vervoort, J.D., Gillet, P., Albarède, F., 2008a. The case for old basaltic shergottites. Earth Planet. Sci. Lett. 266, 105–124.

Bouvier, A., Vervoort, J.D., Patchett, P.J., 2008b. The Lu–Hf and Sm–Nd isotopic composition of CHUR: constraints from unequilibrated chondrites and implications for the bulk composition of terrestrial planets. Earth Planet. Sci. Lett. 273, 48–57.

Boyet, M., Carlson, R.W., 2005. ^{142}Nd evidence for early (>4.53 Ga) global differentiation of the silicate Earth. Science 309, 576–581.

Carlson, R.W., Irving, A.J., 2004. Pb–Hf–Sr–Nd isotopic systematics and age of Nakhlite NWA 998. Proc. Lunar Planet. Sc. Conf. XXXV abs. #1442.

Caro, G., Bourdon, B., Halliday, A.N., Quitté, G., 2008. Super-chondritic Sm/Nd ratios in Mars, the Earth and the Moon. Nature 452, 336–339.

Carr, M.H., Crumpler, L.S., Cutts, J.A., Greeley, R., Guest, J.E., Masursky, H., 1977. Martian impact craters and emplacement of ejecta by surface flow. J. Geophys. Res. 82, 4055–4064.

Chen, J.H., Wasserburg, G.J., 1986a. Formation ages and evolution of Shergotty and its parent planet from U–Th–Pb systematics. Geochim. Cosmochim. Acta 50, 955–968.

Chen, J.H., Wasserburg, G.J., 1986b. S (not equal to) N (maybe equal) C. Proc. Lunar Planet. Sci. Conf. XVII, 113–114.

Debaille, V., Brandon, A.D., Yin, Q.-Z., Jacobsen, B., 2007. Coupled ^{142}Nd–^{143}Nd evidence for a protracted magma ocean in Mars. Nature. 450, 525–528.

Elkins-Tanton, L.T., Zaranek, S.E., Parmentier, E.M., Hess, P.C., 2005. Early magnetic field and magmatic activity on Mars from magma ocean cumulate overturn. Earth Planet. Sci. Lett. 236, 1–12.

Fairen, A.G., Fernandez-Remolar, D., Dohm, J.M., Baker, V.M., Amils, R., 2004. Inhibition of carbonate synthesis in acidic ocean on Early Mars. Nature 431, 423–426.

Foley, C.N., Wadhwa, M., Borg, L.E., Janney, P.E., Hines, R., Grove, T.L., 2005. The early differenciation history of Mars from ^{182}W–^{142}Nd isotope systematics in the SNC meteorites. Geochim. Cosmochim. Acta 69, 4557–4571.

Frey, H.V., 2006. Impact constraints on the age and origin of the lowlands of Mars. Geophys. Res. Lett. 33. doi:10.1029/2005GL024484.

Frey, H.V., Roark, J.H., Shockey, K.M., Frey, E.L., Sakimoto, S.E.H., 2002. Ancient lowlands on Mars. Geophys. Res. Lett. 29, 1384–1387.

Fritz, J., Greshake, A., Stöffler, D., 2007. The Martian meteorite paradox: climatic influence on impact ejection from Mars? Earth Planet.Sci. Lett. 256, 55–60.

Gaffney, A.M., Borg, L.E., Connelly, J., 2007. Uranium–lead isotope systematics of Mars inferred from the basaltic shergottite QUE 94201. Geochim. Cosmochim. Acta 71, 5016–5031.

Galer, S.J.G., O'Nions, R.K., 1985. Residence time of thorium, uranium and lead in the mantle with implications for mantle convection. Nature 316, 778–782.

Greenwood, J.P., Itoh, S., Sakamoto, N., Vicenzi, E.P., Yurimoto, H., 2008. Hydrogen isotope evidence for loss of water from Mars through time. Geophys. Res. Lett. 35. doi:10.1029/2007GL032721.

Hartmann, W.K., 1970. Preliminary note on lunar cratering rates and absolute time-scales. Icarus 12, 131–133.

Hartmann, W.K., Neukum, G., 2001. Cratering chronology and the evolution of Mars. Space Sci. Rev. 96, 165–194.

Hartmann, W.K., Barlow, N.G., 2006. Nature of the Martian uplands: effect on Martian meteorite age distribution and secondary cratering. Meteorit. Planet. Sci. 41, 1453–1467.

Jagoutz, E., 1991. Chronology of SNC meteorites. Space Sci. Rev. 56, 13–22.

Jagoutz, E., Sorowka, A., Vogel, J.D., Wanke, H., 1994. ALH 84001: alien or progenitor of the SNC family? Meteoritics 29, 478–479.

Jones, J.H., 1986. A discussion of isotopic systematics and mineral zoning in the shergottites: evidence for a 180 m.y. igneous crystallization age. Geochim. Cosmochim. Acta 50, 969–977.

Jones, J.H., 2003. Constraints on the structure of the martian interior determined from the chemical and isotopic systematics of SNC meteorites. Meteorit. Planet. Sci. 38, 1807–1814.

Kleine, T., Mezger, K., Münker, C., Palme, H., Bischoff, A., 2004. ^{182}Hf–^{182}W isotope systematics of chondrites, eucrites, and martian meteorites: chronology of core formation and early mantle differentiation in Vesta and Mars. Geochim. Cosmochim. Acta 68, 2935–2946.

Lecuyer, C., Reynard, B., Grandjean, P., 2004. Rare earth element evolution of Phanerozoic seawater recorded in biogenic apatites. Chem. Geol. 204, 63–102.

Leshin Watson, L., Hutcheon, I.D., Epstein, S., Stolper, E.M., 1994. Water on Mars: clues from Deuterium/Hydrogen and water contents of hydrous phases in SNC meteorites. Science 265, 86–90.

Longhi, J., 1991. Complex magmatic processes on Mars: inferences from the SNC meteorites. Proc. Lunar Planet. Sci. Conf. 21, 695–709.

Ludwig, K.R., 2008. Isoplot/Ex version 3.64. A Geochronological Toolkit for Microsoft Excel., Berkeley Geochronology Center. March 17.

Manhès, G., Allègre, C.J., Duprè, B., Hamelin, B., 1979. Lead–lead systematics, the 'age of the earth' and the chemical evolution of our planet in a new representation space. Geochim. Cosmichim. Acta 44, 91–104.

Misawa, K., Shih, C.-Y., Reese, Y., Nyquist, L.E., Barrat, J.-A., 2005. Rb–Sr and Sm–Nd isotopic systematics of NWA 2737 chassignite. Meteorit. Planet. Sci. 40 abs. #5200.

Misawa, K., Shih, C., Bogard, D.D., Nyquist, L.E., 2006. Rb–Sr, Sm–Nd and Ar–Ar isotopic systematics of Martian dunite Chassigny. Earth Planet. Sci. Lett. 246, 90–101.

Nakamura, N., Unruh, D.M., Tatsumoto, M., 1982. Origin and evolution of the Nakhla meteorite inferred from the Sm–Nd and U–Pb systematics and REE, Ba, Sr, Rb and K abundances. Geochim. Cosmochim. Acta 46, 1555–1573.

Nesvorny, D., Vokrouhlicky, D., Bottke, W.F., 2005. The breakup of a main-belt Asteroid 450 thousand years ago. Science 312, 1490.

Neukum, G., Wise, D.U., 1976. Mars—a standard crater curve and possible new time scale. Science 194, 1381–1387.

Nyquist, L.E., Bogard, D.D., Garrison, D.H., Bansal, B.M., Wiesmann, H., Shih, C.-Y., 1991. Thermal resetting of radiometric ages. I: experimental investigation. Proc. Lunar Planet. Sci. Conf. XXII abs. #985.

Nyquist, L.E., Bansal, B., Wiesmann, H., Shih, C.-Y., 1995. Martians young and old: zagami and ALH 84001. Proc. Lunar Planet. Sci. Conf. XXVI, 1065–1066.

Nyquist, L.E., Bogard, D.D., Shih, C., Greshake, A., Stöffler, D., Eugster, O., 2001. Ages and geologic histories of martian meteorites. Space Sci. Rev. 96, 105–164.

Righter, K., 2008. The Lunar meteorite compendium. http://www-curator.jsc.nasa.gov/antmet/lmc/index.cfm Astromaterials Research & Exploration Science (ARES). Lyndon B. Johnson Space Center, Houston, Texas.

Righter, K., Shearer, C.K., 2003. Magmatic fractionation of Hf and W: constraints on the timing of core formation and differentiation in the Moon and Mars. Geochim. Cosmochim. Acta 67, 2497–2507.

Rocholl, A., Jochum, K.P., 1993. Th, U and other trace elements in carbonaceous chondrites: implications for the terrestrial and solar-system Th/U ratios. Earth Planet. Sci. Lett. 117, 265–278.

Rosholt, J.N., Bartel, A.J., 1969. Uranium, thorium, and lead systematics in Granite Mountains, Wyoming. Earth Planet. Sci. Lett. 7, 141–147.

Soderblom, L.A., Condit, C.D., West, R.A., Herman, B.M., Kreidler, A.-D.T., 1974. Martian planetwide crater distributions: implications for geologic history and surface processes. Icarus 22, 239–263.

Sokol, A.K., Fernandes, V.A., Schulz, T., Bischoff, A., Burgess, R., Clayton, R.N., Münker, C., Nishiizumi, K., Palme, H., Schultz, L., Weckwerth, G., Mezger, K., Horstmann, M., 2008. Geochemistry, petrology and ages of the lunar meteorites Kalahari 008 and 009: new constraints on early lunar evolution. Geochim. Cosmichim. Acta 72, 4845–4873.

Stacey, J.S., Kramers, J.D., 1975. Approximation of terrestrial lead isotope evolution by a two-stage model. Earth Planet. Sci. Lett. 26, 207–221.

Symes, S.J., Borg, L.E., Shearer, C.K., Irving, A.J., 2008. The age of the martian meteorite Northwest Africa 1195 and the differentiation history of the shergottites. Geochim. Cosmochim. Acta 72, 1696–1710.

Tatsumoto, M., Knight, R.J., Allegre, C.J., 1973. Time differences in the formation of meteorites as determined from the ratio of lead 207 to lead 206. Science 180, 1279–1283.

Taylor, S.R., Jakes, P., 1974. Geochemical zoning in the Moon. Proc. Lunar Planet. Sci. Conf. V., 786–789.

Tera, F., Wasserburg, G.J., 1974. U–Th–Pb systematics on lunar rocks and inferences about lunar evolution and the age of the Moon. Proc. Lunar Planet. Sci. Conf. 2, 1571–1599.

Tera, F., Wasserburg, G.J., 1975. The evolution and history of Mare Basalts as inferred from U–Th–Pb systematics. Proc. Lunar Planet. Sci. Conf. VI abs. #807.

Tera, F., Carlson, R.W., Boctor, N.Z., 1997. Radiometric ages of basaltic achondrites and their relation to the early history of the Solar System. Geochim. Cosmochim. Acta 61, 1713–1731.

Wadhwa, M., McSween Jr., H.Y., Crozaz, G., 1994. Petrogenesis of shergottite meteorites inferred from minor and trace element microdistributions. Geochim. Cosmochim. Acta 58, 4213–4229.

Werner, S.C., 2008. The early martian evolution—constraints from basin formation ages. Icarus 195, 45–60.